Supporting Information

Construction of matchstick-shaped Au@ZnO@SiO_2-ICG Janus nanomotor for light-triggered synergistic antibacterial therapy

Xuan Liu, Huaxiao Liu, Jinzha Zhang, Yijie Hao, Hongna Yang, Wenbo Zhao and Chun Mao*

National and Local Joint Engineering Research Center of Biomedical Functional Materials, School of Chemistry and Materials Science, Nanjing Normal University, Nanjing 210023, P. R. China.
E-mail: zhaowenbo@njnu.edu.cn

Experimental Section

***Materials*:** All chemical reagents used in this experiment are of analytical grade and no further purification is required. Tetrachloroauric acid trihydrate ($HAuCl_4 \cdot 3H_2O$) was purchased from Kefeng Industrial Co., Ltd. Zinc acetate dihydrate, oleylamine (OAm), 1,3-diphenylisobenzofuran (DPBF), 3-aminopropyltriethoxysilane (APTES), 2-methoxy-(polyethoxy Yl)-propyltrimethoxysilane (mPEG-Silane) and dimethyl sulfoxide (DMSO) were purchased from Aladdin Reagent Co., Ltd. Tetraethyl orthosilicate (TEOS), benzyl alcohol (BA), glutaraldehyde (25 %), ammonia, methylene blue, n-hexane, cyclohexane, and absolute ethanol were all purchased from Sinopharm Chemical Reagent Co., Ltd. (Shanghai, China). Cy5-NHS was purchased from Apexbio Technology Co., Ltd., methylthiazolyltetrazole (MTT) was purchased from Shanghai Shenggong Company, and embryonic bovine serum was purchased from Zhejiang Tianhang Biotechnology Co., Ltd. Calcein AM, propidium iodide (PI), PBS, and DMEM were purchased from Jiangsu KGI Biotechnology Co., Ltd. Escherichia coli and

Staphylococcus aureus were provided by Nanjing Tianjia Testing Service Co., Ltd., and nutrient agar was purchased from Guangdong Huankai Microbial Technology Co., Ltd. Lgepal CO-520 (ALDRICH). 2,7-Dichlorofluorescein diacetate (DCFH-DA) was purchased from SIGMA ALDRICH, deionized water is used for all reactions and cleaning processes.

***Apparatus and Measurements*:** The TEM of the nanoparticles was taken on the H-7650 transmission electron microscope. The photothermal of the material is tested by 808 nm laser (MDL-III-808NM(FC)) and thermal imager (Fotric 226s). The dynamic light scattering (DLS) and Zeta potential experiments were carried out, and the tests were carried out on the Nano ZS 90. A Ti-E-A1R confocal laser scanning microscope was used to take confocal luminescence images. Perform infrared spectroscopy tests on Tensor 27 Fourier infrared spectrometer. The UV-vis test was performed on the Cary 50 UV-Vis spectrophotometer. Use an X-ray diffractometer (D/max 2500VL / PC) to detect X-ray diffraction (XRD) patterns.

Evaluation of extracellular ROS generation: The production of singlet oxygen ($^1O_2$) is detected by 1,3-diphenylisobenzofuran (DPBF). DPBF can irreversibly react with $^1O_2$, resulting in a decrease in the absorbance of DPBF at 420 nm. The DPBF solution (10 mM, 20 μL) was added to the Au@ZnO@SiO_2-ICG (120 μg mL^{-1}, 2 mL) solution. Then the mixture was irradiated under 808 nm laser (1.5 W cm^{-2}) for various time periods (0, 2, 4, 6 min). No material group served as a blank control. Finally, the absorbance of DPBF at 420 nm at different times was detected by UV-Vis absorption spectroscopy.

In order to determine the photocatalytic reaction and the ability of Au@ZnO@SiO_2-ICG to generate hydroxyl radicals (•OH) under ultraviolet light irradiation, the Au@ZnO@SiO_2-ICG (120 μg mL^{-1}, 2 mL) solution was combined with methylene blue (MB, 30 μg mL^{-1}) was mixed and irradiated under ultraviolet light (UV, 31-40 W) for various time periods (0, 2, 4, 6 min). No

material group served as a blank control. Finally, the absorbance of MB at 665 nm at different times was detected by UV-Vis absorption spectroscopy.

In vitro measurement of laser-induced photothermal (PTT) effect of Au@ZnO@SiO_2-ICG: The photothermal effects of Au@ZnO@SiO_2-ICG nanocomposites with different concentrations were studied. A 808 nm laser was used as the light source, and a thermal imager was used to record the photothermal image of the Au@ZnO@SiO_2-ICG aqueous solution.

Bacteria morphological characteristics: In order to better evaluate how the Au@ZnO@SiO_2-ICG nanomotor interacts with the bacteria, the E. coli and the nanomotor were incubated for 2 h and irradiated under NIR light for different times. After treatment, the bacteria were washed twice with PBS, and the bacteria were used After diluting a 2.5 % glutaraldehyde solution and fixing it in a refrigerator at 4 ℃ for 12 h, the bacterial suspension was dropped on a carbon-supported copper net and air-dried, and then different concentrations of ethanol (30 %, 50 %, 70 %, 80 %, 90 %, 100 %) dehydration treatment for 5 minutes. Untreated bacteria liquid was used as a blank control. Finally, use a transmission electron microscope to observe the morphology of the bacteria.

Cell compatibility of Au@ZnO@SiO_2-ICG: The MTT assay was used to determine the viability of the cells. The MCF-7 cells were seeded in a 96-well plate and incubated overnight at 37 °C in an atmosphere containing 5% CO_2 to allow the cells to attach to the wells. Then, add 150 μL of a new medium with different concentrations of Au@ZnO@SiO_2-ICG, and incubate with the cells for 24 hours. Add 20 μL of MTT solution to each well. After incubating for 4 hours, remove the medium and MTT, add 100 μL of DMSO to each well, and measure the absorbance of the cells at 570 nm using a microplate reader.

Live-Dead Cell Staining: In order to visually observe the bacterial status, the bacteria were stained with calcein AM and propidium iodide (PI) to further characterize the PTT/PDT performance. In short, Staphylococcus aureus and Escherichia coli were incubated with Au@ZnO@SiO_2-ICG (120 μg mL^{-1}) at a density of 10^8 CFU mL^{-1} for 1 hour, and then 808 nm laser (1.5 W cm^{-2}) was used respectively. Irradiate for 6 minutes, UV light (31-40 W) for 6 minutes, and irradiate both. After staining each group of bacteria with AM-PI double staining reagent, incubate at 37°C for 15 min, and observe live/dead bacteria with green/red fluorescence using a laser scanning confocal microscope.

Evaluation of intracellular ROS generation: Use 2,7-dichlorofluorescein diacetate (DCFH-DA) to detect the production of ROS in bacteria, which can be easily oxidized by ROS to 2,7-dichlorofluorescein (DCF) and emit green fluorescence. Inoculate 100 μL (10^8 CFU mL^{-1}) of the bacterial suspension of Staphylococcus aureus and Escherichia coli into a petri dish, and incubate with Au@ZnO@SiO_2-ICG for 1 hour, then add the DCFH-DA probe to the culture and incubate with bacteria for 30 minutes. Then, they were exposed to 808 nm laser (1.5 W cm^{-2}, 6 minutes), ultraviolet light (31-40 W, 6 minutes), and irradiated under both types of light. Observe the distribution of ROS with a confocal laser microscope.

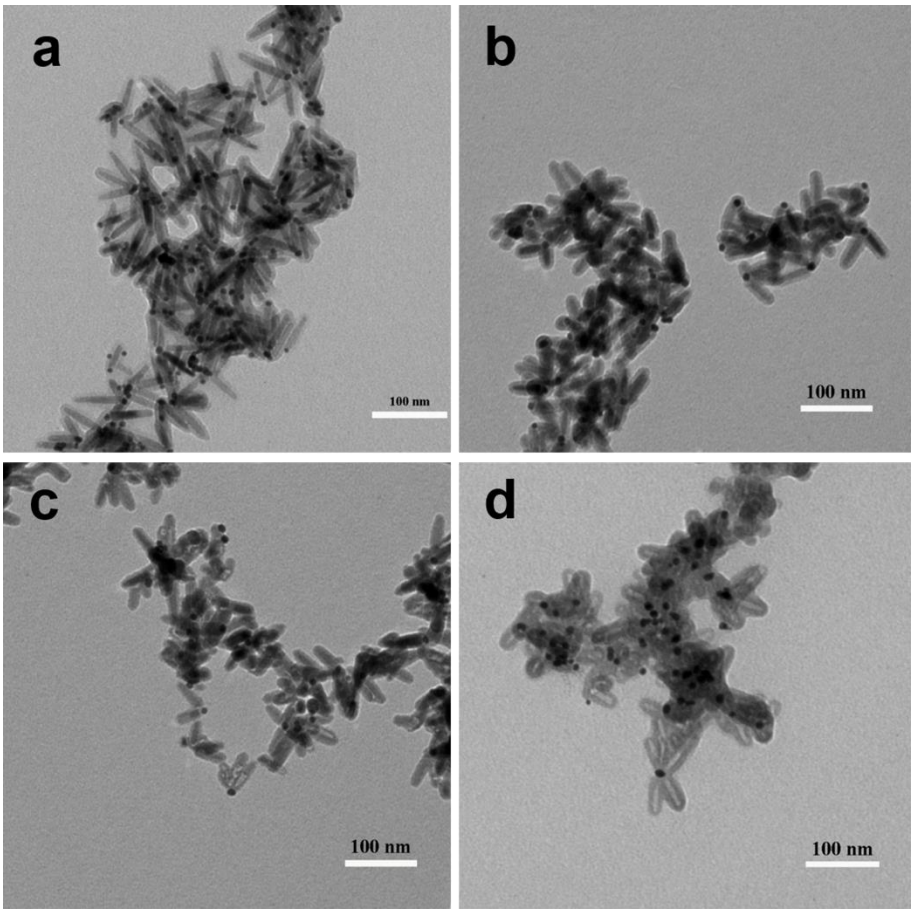

Fig. S1. a) TEM image of Au@ZnO@SiO_2-ICG. b) when the alkali dosage is increased to 130 μL, the thickness of the formed SiO_2 shell is about 6-7 nm. when the alkali is excessive, there are damaged c) and hollow d) Janus structure.

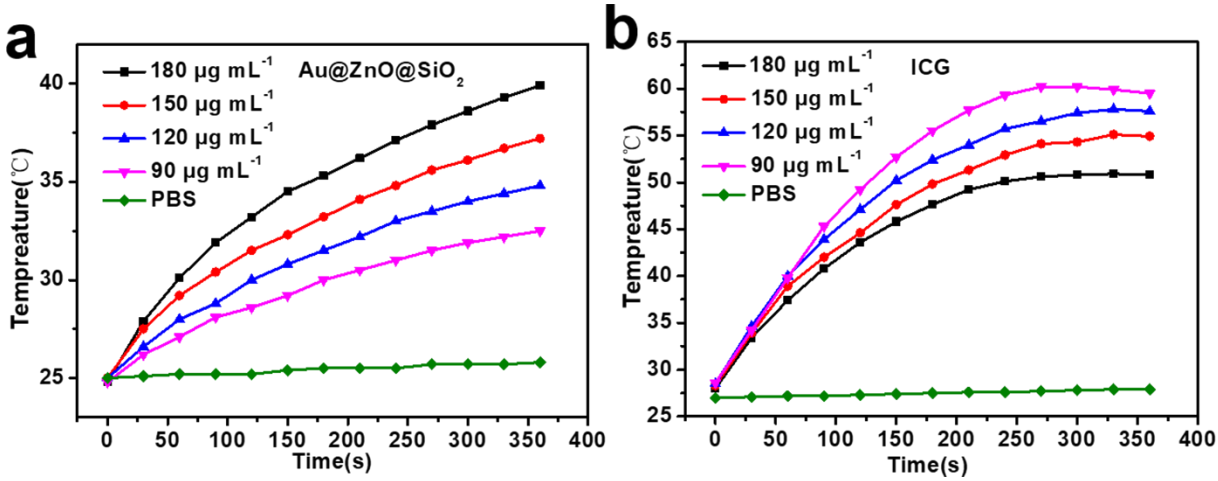

Fig. S2. Temperature elevation curves of a) Au@ZnO@SiO_2 and b) ICG with different concentrations under 808 nm NIR laser (1.5 W cm^{-2}).

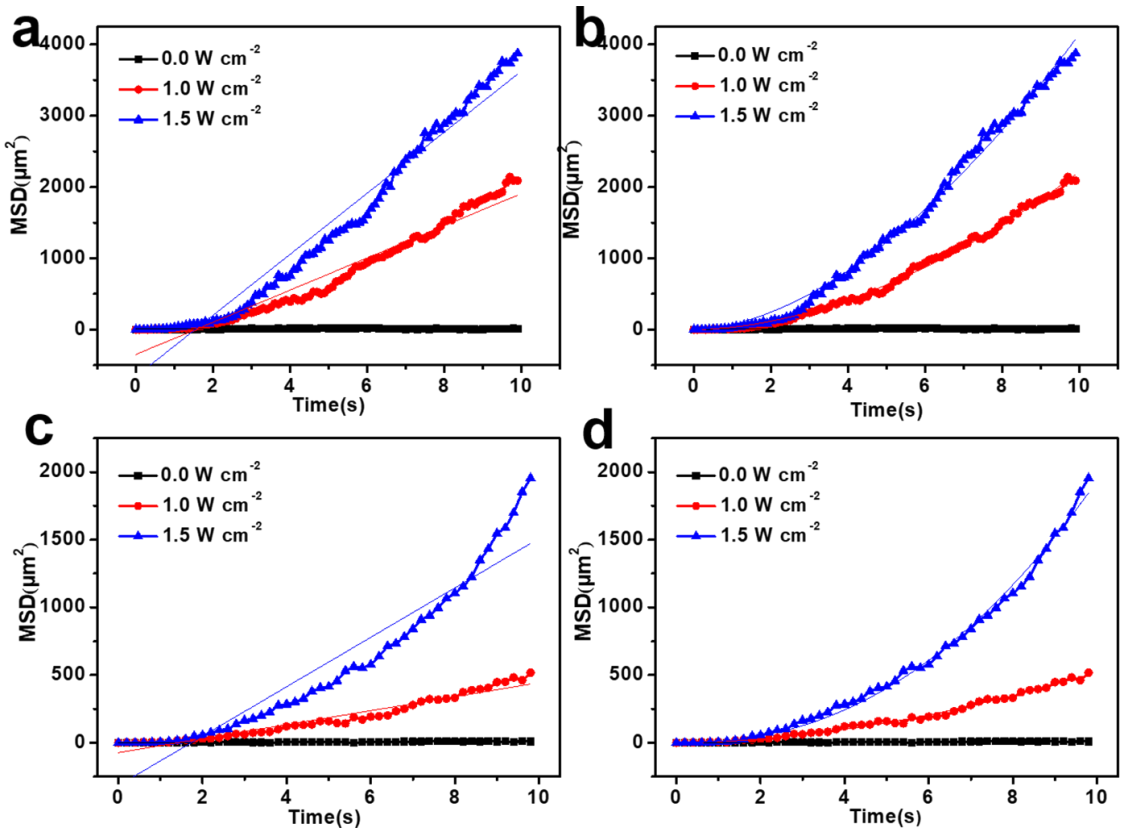

Fig. S3. a) Linear (y = a + bx) fitting. b) Power function ($y=ax^b$) fitting of the MSD graphs of Au@ZnO@SiO_2 in aqueous solution under different near-infrared power densities. c) Linear (y = a + bx) fitting. d) power function ($y=ax^b$) fitting of MSD graphs of Au@ZnO@SiO_2 in bacterial solution under different near-infrared power densities.

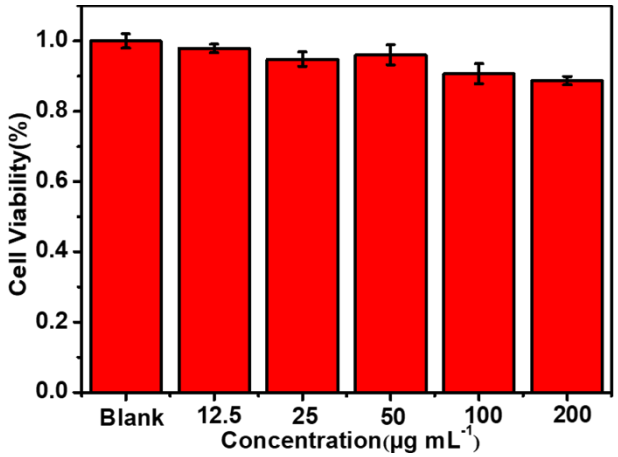

Fig. S4. The cytotoxicity graph of Au@ZnO@SiO_2-ICG at different concentrations (0, 12.5, 25, 50, 100, and 200 μg mL^{-1}) treated with MCF-7 cells.

Table S1. Fitting parameters of the linear function (y = a + bx) of the MSD diagram of Au@ZnO@SiO_2 nanomotor in aqueous solution at different near-infrared power densities.

Power density (W cm^{-2})	R^2	a	b
0	0.08473	5.38659	0.65071
1	0.95439	-348.41832	225.81829
1.5	0.96087	-656.47105	428.51288

Table S2. Fitting parameters of the parabolic function ($y = ax^2 + bx + c$) of the MSD diagram of Au@ZnO@SiO_2 nanomotor in aqueous solution at different near-infrared power densities.

Power density (W cm^{-2})	R^2	a	b	c
0	0.50932	-0.53621	5.95921	-3.28397
1	0.99607	18.19077	45.72967	-54.27357
1.5	0.99397	30.6725	124.85509	-160.49666

Table S3. Fitting parameters of the power function ($y=ax^b$) of the MSD diagram of Au@ZnO@SiO_2 nanomotor in aqueous solution at different near-infrared power densities.

Power density (W cm^{-2})	R^2	a	b
0	0.17012	5.49127	0.32668
1	0.99622	33.87382	1.81557
1.5	0.99403	72.74826	1.75601

Table S4. Fitting parameters of the linear function (y = a + bx) of the MSD diagram of Au@ZnO@SiO_2 nanomotor in bacterial solution at different near-infrared power densities.

Power density (W cm^{-2})	R^2	a	b
0	0.77145	0.50609	1.06966
1	0.94276	-72.25468	51.67157
1.5	0.9032	-315.57799	182.48553

Table S5. Fitting parameters of the parabolic function ($y = ax^2 + bx + c$) of the MSD diagram of Au@ZnO@SiO_2 nanomotor in bacterial solution at different near-infrared power densities.

Power density (W cm^{-2})	R^2	a	b	c
0	0.76756	-0.01432	1.20997	0.28159
1	0.99312	4.5849	6.73957	-0.36348
1.5	0.99416	22.20828	-35.15563	32.64787

Table S6. Fitting parameters of the power function ($y=ax^b$) of the MSD diagram of Au@ZnO@SiO_2 nanomotor in bacterial solution at different near-infrared power densities.

Power density (W cm^{-2})	R^2	a	b
0	0.75891	1.45509	0.87782
1	0.99271	7.98289	1.81546
1.5	0.99539	10.6221	2.25994

R^2 is coefficient of determination.